

Understanding electron-molecular vibrational coupling in organic molecular solids: Experimental evidence for strong coupling of the 890-cm⁻¹ mode in ET-based materials

J. L. Musfeldt,¹ R. Świetlik,² I. Olejniczak,² J. E. Eldridge,³ and U. Geiser⁴

¹Department of Chemistry, University of Tennessee, Knoxville, Tennessee, 37996, USA

²Institute of Molecular Physics, Polish Academy of Sciences, Smoluchowskiego 17, 60-179 Poznań, Poland

³Department of Physics and Astronomy, University of British Columbia, Vancouver, B.C. V6T 1Z1, Canada

⁴Materials Science Division, Argonne National Laboratory, Argonne, Illinois 60439, USA

(Received 13 January 2005; published 11 July 2005)

We report a detailed analysis of the vibrational response of several model organic molecular conductors and superconductors. We demonstrate that the 890 cm⁻¹ mode, originally assigned and discussed as ν_{60} (B_{3g}) in the D_{2h} point group symmetry, displays an unusual sensitivity to both chemical and physical tuning for a wide variety of materials. Based upon the analysis of these combined spectral results as well as an assessment of the local molecular and crystallographic structure, we find ample experimental evidence for vibronic coupling of the 890 cm⁻¹ mode. This mode is not vibronically active within the planar dynamics framework, and its presence in the optical conductivity demonstrates that local symmetry breaking effects are important in layered organic molecular materials.

DOI: [10.1103/PhysRevB.72.014516](https://doi.org/10.1103/PhysRevB.72.014516)

PACS number(s): 78.20.-e, 78.30.-j, 63.20.Kr, 74.70.Kn

I. INTRODUCTION

There have been many theoretical efforts to understand the electron-molecular vibration (EMV) interaction in molecular solids.¹⁻⁶ From symmetry considerations, only totally symmetric modes couple with the electronic system.⁷ Activated modes are typically characterized by their strength and polarization dependence, a marked redshift compared to the unperturbed resonance frequency in the Raman spectrum, and unusual sensitivity to various phase transitions. In salts based upon the bis(ethylenedithio)tetrathiafulvalene (ET) molecule, e.g., κ -(ET)₂Cu(SCN)₂, twelve vibrational modes of A_g symmetry are available for activation, assuming a planar (D_{2h}) point group symmetry.^{8,9} Normally infrared active modes of B_u symmetry also appear in the infrared spectrum, but with weaker intensity. The 890 cm⁻¹ mode has attracted attention as a major feature in the optical conductivity spectrum.¹⁰ It is traditionally assigned as ν_{60} (B_{3g}) in the D_{2h} point group picture.¹⁰⁻¹² Several scenarios, including the possibility of nontotally symmetric EMV-like coupling and/or nonlinear coupling effects,^{7,10,13-15} have been proposed to account for the unexpected appearance and behavior of this mode. The impact of local molecular symmetry, ethylene group distortion, and solid state structure on the dynamics is, however, relatively unexplored.

In order to address continuing questions on the nature of the EMV interaction in organic molecular solids, we have drawn together compelling crystal and spectral data for selected low-dimensional ET-based solids. Notably, the ethylene end groups in the ET building block molecule are never flat, and even the conjugated portion of the molecule is subject to symmetry-lowering local distortions caused by charge and crystal interactions. Local distortions have recently been shown to have important implications for the vibrational properties, with a completely new set of modes present when weak local distortions are taken into account.¹⁶ In particular,

a totally symmetric “ring breathing mode” is predicted at 890 cm⁻¹. From an experimental point of view, we find that the 890 cm⁻¹ mode displays an unusual sensitivity to temperature, anion modification, application of a magnetic field, and phase transitions driven by physical tuning. This sensitivity supports the predicted EMV activation of the 890 cm⁻¹ feature.¹⁶ Similar results might be anticipated in other molecular materials with flexible building block units.

II. RESULTS AND DISCUSSION

A. Structural symmetry-breaking in ET-based molecular solids

Figure 1 shows a comprehensive view of the symmetry relationships in the ET molecule with various ethylene group distortions. The scheme summarizes how local molecular structure can distort from planar D_{2h} symmetry in the real crystallographic environment. The two top-level distortions are the D_2 and C_{2h} subgroups, corresponding to staggered and eclipsed local geometries, respectively. Subsequent effects can reduce the local symmetry even more, and in the solid state, most organic molecular solids display a formal C_1 local symmetry. The center of the ET building block molecule is relatively unaffected by this local molecular distortion (as long as the partial charge of the molecule remains the same), so vibrational modes that involve mostly the central part of the molecule (such as the C=C stretch) will be fairly unmodified, whereas modes involving the outer portions of the molecule will be more substantially modified by the reduced symmetry. The crystal structures of the salts discussed in this paper have been previously determined.¹⁷ By bringing this data together, we seek to emphasize out-of-plane molecular distortions and the implications for vibrational properties, rather than simple packing arrangements.

κ -(ET)₂X compounds (X=Cu(SCN)₂, Cu[N(CN)₂]Br, and Cu[N(CN)₂]Cl) are three of the most widely studied organic superconductors. They are considered to be quasi-

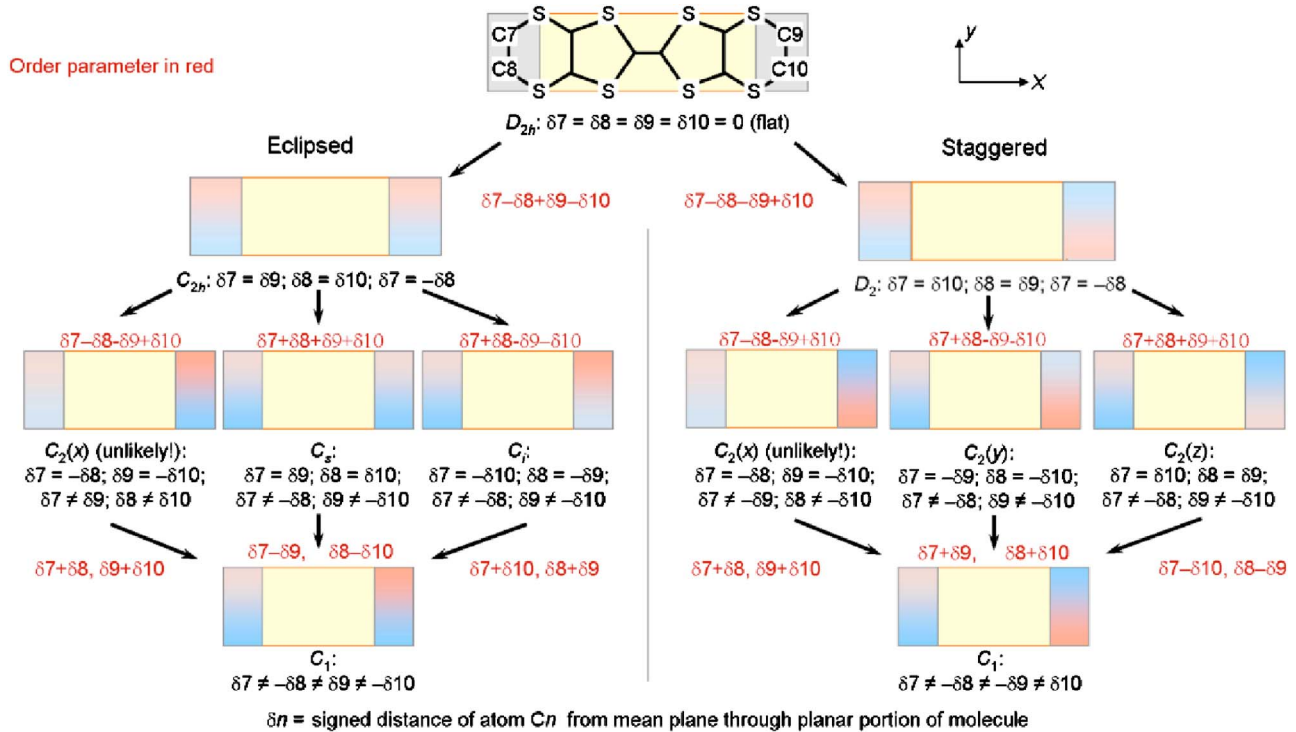


FIG. 1. (Color online) Symmetry relationships in the ET molecule with different ethylene group distortions. The principle distortions of the planar (D_{2h}) molecule are to either C_{2h} (eclipsed) or D_2 (staggered) forms. Lower symmetry structures are shown as well. The ethylene end groups are schematically represented as color (greyscale) gradients, where red (dark grey) and blue (medium-dark grey) indicate the displacements of the carbon atoms to opposite sides of the drawing plane (n values). The intensity of the color is a measure of the amount of distortion from planarity, although for symmetry purposes, it is only relevant whether the displacements are equal in magnitude or not. Thus, bright red and bright blue (or pale red and pale blue) signify equal but opposite displacements, whereas bright and pale are unequal, regardless of color. The grey shading (for the printed version) shows the same distortions.

isostructural because of their similar molecular packing arrangements. Consideration of local distortion, however, emphasizes their differences. As shown in Fig. 1, the two main deviations from planarity are eclipsed (C_{2h}) and

(D_2). The molecular symmetries in κ -(ET) $_2$ Cu[N(CN) $_2$]Br and κ -(ET) $_2$ Cu[N(CN) $_2$]Cl are lower than eclipsed, and the molecular symmetries of κ -(ET) $_2$ Cu(SCN) $_2$ are lower than staggered.^{18–21} We quantify these molecular distortions in

TABLE I. Displacements (in Å) of the ethylene end group carbon atom positions from the least-squares plane through the conjugated portion of the ET molecule for three model κ -phase organic superconductors, calculated from the coordinates published in the listed references. Relevant symmetry-adapted linear combinations (see Fig. 1) are also shown.

	κ -(ET) $_2$ Cu(NCS) $_2$ 118 K		κ -(ET) $_2$ Cu[N(CN) $_2$]Br 127 K	κ -(ET) $_2$ Cu[N(CN) $_2$]Cl 127 K
Temperature				
	Mol. 1	Mol. 2		
δ_7	-0.36	-0.63	-0.02	+0.00
δ_8	+0.18	+0.08	-0.77	-0.80
δ_9	+0.02	+0.07	+0.36	+0.36
δ_{10}	-0.68	-0.64	-0.43	-0.41
Conformation	staggered	staggered	eclipsed	eclipsed
$\delta_7 - \delta_8 + \delta_9 - \delta_{10}$	+0.16	+0.00	+1.54	+1.57
$\delta_7 - \delta_8 - \delta_9 + \delta_{10}$	-1.24	-1.42	-0.04	+0.03
$\delta_7 + \delta_8 + \delta_9 + \delta_{10}$	-0.84	-1.12	-0.86	-0.85
$\delta_7 + \delta_8 - \delta_9 - \delta_{10}$	+0.48	+0.02	-0.72	-0.75
Reference	21		18	18

TABLE II. Displacements (in Å) of the ethylene end group carbon atom positions from the least-squares plane through the conjugated portion of the ET molecule for the “tunable anion” materials, calculated from the coordinates published in the listed references. The presence of disordered ethylene groups is marked as “dis.” Relevant symmetry-adapted linear combinations (see Fig. 1) are also shown.

(ET) ₂ SF ₅ RSO ₃	R=CH ₂ CF ₂		R=CHF ₂		R=CHF		R=CH ₂	
Temperature	123 K		150 K		298 K		298 K	
	Mol. 1	Mol. 2	Mol. 1	Mol. 2	Mol. 1	Mol. 2	Mol. 1	Mol. 2
δ_7	-0.41	-0.69	+0.11	-0.78	+0.37	-0.36	-0.42	+0.27
δ_8	+0.34	+0.23	-0.65	+0.03	-0.30	+0.31	+0.30	-0.39
δ_9	-0.84	-0.13	-0.79	+0.14	+0.16	-0.21	dis	+0.39
δ_{10}	+0.04	+0.60	+0.03	-0.68	-0.67	+0.70	dis	-0.50
Conformation	eclipsed	eclipsed	staggered	staggered	eclipsed	eclipsed	dis	eclipsed
$\delta_7 - \delta_8 + \delta_9 - \delta_{10}$	-1.63	-1.65	-0.06	+0.01	+1.50	-1.58	n/a	+1.55
$\delta_7 - \delta_8 - \delta_9 + \delta_{10}$	+0.05	-0.19	+1.58	-1.63	-0.16	+0.24	n/a	-0.23
$\delta_7 + \delta_8 + \delta_9 + \delta_{10}$	-0.87	+0.01	-1.30	-1.29	-0.44	+0.44	n/a	-0.23
$\delta_7 + \delta_8 - \delta_9 - \delta_{10}$	+0.73	-0.93	+0.22	-0.21	+0.58	-0.54	n/a	-0.01
Reference	24		25		26		26	

Table I. Note that ethylene group twisting with respect to the ET plane constitutes a local deformity, not a long-range change in the unit cell. Small differences in ethylene group disorder may be present as well.²²

In all of the β'' -(ET)₂SF₅RSO₃ salts discussed in this paper, two crystallographically independent, albeit coplanar, molecules with approximately parallel long molecular axes, are present.^{23–26} As an example, the displacements of the ethylene groups from the molecular plane, and relevant linear combinations thereof are listed in Table II. As can be seen from these values, in almost all of these salts, the distortions lead to a symmetry reduction to trivial (C_1) local symmetry. Two exceptions can be found, however, where the local symmetry is approximated by one of the more symmetrical point groups. (1) In molecule 2 of the superconductor β'' -(ET)₂SF₅CH₂CF₂SO₃ $\delta_7 \approx -\delta_{10}$ and $\delta_8 \approx -\delta_9$, thus the symmetry on this molecule is approximately C_i . (2) In molecule 2 of β'' -(ET)₂SF₅CHF₂SO₃ $\delta_7 \approx \delta_{10}$ and $\delta_8 \approx \delta_9$, leading to approximate local symmetry $C_2(z)$.

κ -(Et₄N)(ET)₄Co(CN)₆·3H₂O is isostructural with its Fe analog at 300 K.^{27,28} Here, crystallographically independent ET molecules are arranged into typical κ -type layers of approximately orthogonal dimers. Inversion centers are located between the molecules constituting a dimer, but no crystallographic symmetry elements are contained within the molecules. The molecule labeled as “A” by the authors^{27,28} is strongly deformed from planarity. Both carbon atoms of one of the ethylene end groups are located on the same side of the conjugated portion of the molecule. The central portion of the molecule is bowed as well. Molecule “B” is more planar, and the ethylene groups adopt a staggered conformation, ideally of D_2 symmetry. The long axis of molecules “A” and “B” are approximately parallel to each other. There is a low-temperature cell-doubling transition that likely involves tetraethylammonium cation ordering and charge disproportionation.^{27–29}

B. Vibronic activation of the 890 cm⁻¹ mode

The vibrational response of various organic building block molecules has been extensively investigated within the assumption of a planar (D_{2h}) building block molecule.^{8,9} The observation and detailed understanding of local symmetry breaking in the solid state (Fig. 1, Tables I and II) provides an opportunity to revisit the dynamics in molecular solids, explore the manifestations of this symmetry breaking in the vibrational spectrum, and to test molecular dynamics predictions for reduced symmetry cases.^{16,30–32} We illustrate experimental efforts in this direction using the 890 cm⁻¹ mode as an especially interesting example. Organic superconductors, conductors, semi-conductors, and charge-ordered systems are represented,^{12,29,33–37} as described below.

Figure 2(a) shows the variable temperature optical conductivity of κ -(Et₄N)(ET)₄Co(CN)₆·3H₂O along the c direction.^{29,33} Here, the mode of interest is centered between 874 and 877 cm⁻¹, depending on the temperature (which influences the charge distribution in the conducting ET layers). As a result of probable EMV coupling, the mode is significantly redshifted from its unperturbed position in the Raman response [Fig. 2(b)]. The substantial downshift (16–18 cm⁻¹, depending on the temperature) suggests a large value of the coupling constant g . Another example of the infrared vibronic shift of the 890 cm⁻¹ mode is the 9 cm⁻¹ downshift between infrared and Raman positions of this mode in κ -(ET)₂Cu(SCN)₂.³⁸

The 890 cm⁻¹ mode is known to display strong temperature dependence, and the response of κ -(Et₄N)×(ET)₄Fe(CN)₆·3H₂O [Fig. 2(c)] is a good example.^{29,33} Here, a major band centered at 873 cm⁻¹ is observed at high temperature. A charge redistribution at 150 K modifies this response.²⁹ The low-temperature phase is characterized by a frequency shift, weak splitting of the feature, and reduced oscillator strength. That this peak is so sensitive to the low-temperature charge disproportionation in κ -(Et₄N)

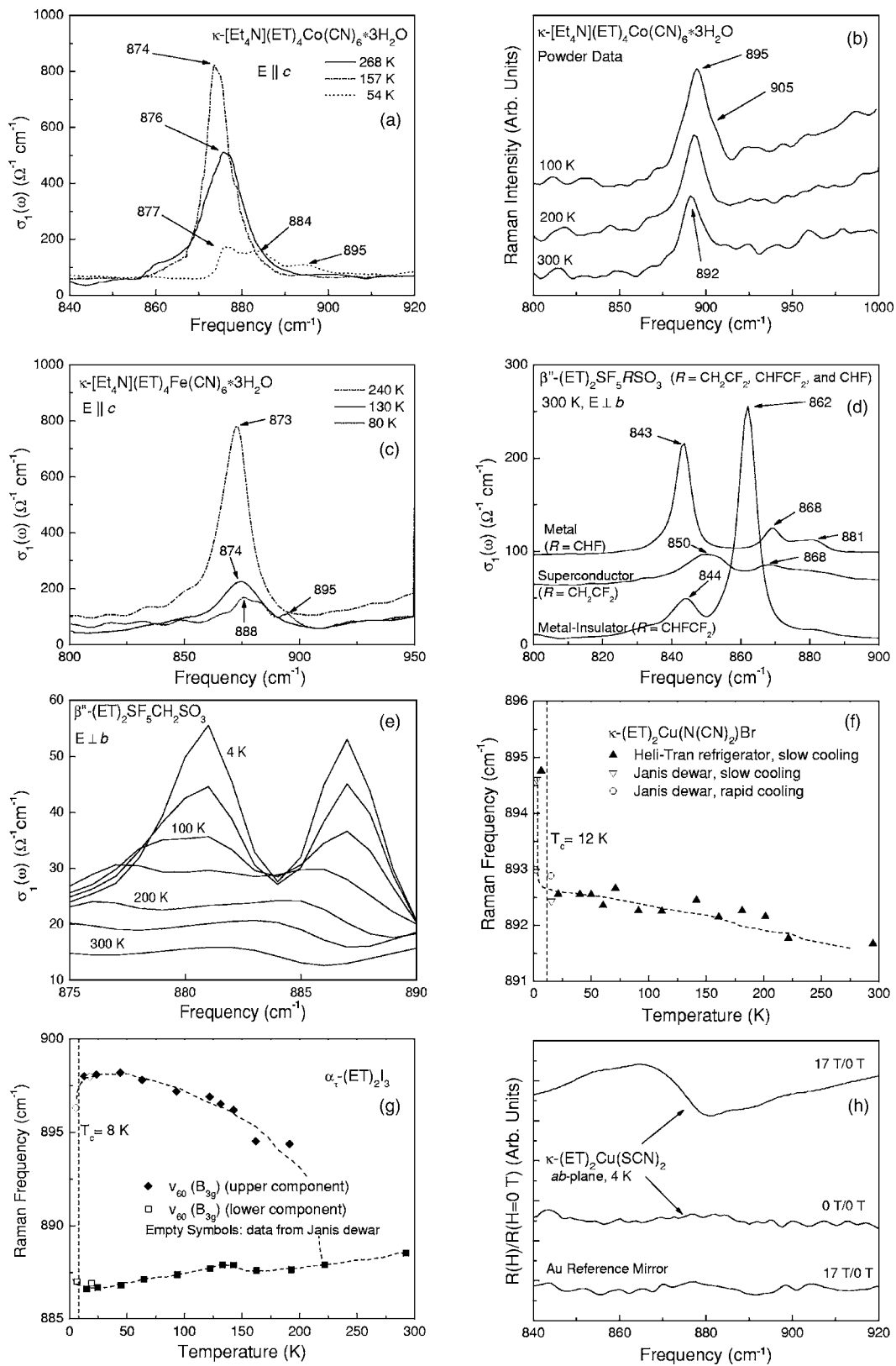


FIG. 2. Close-up views of several spectra that illustrate the unusual sensitivity of the 890 cm⁻¹ mode to physical and chemical tuning effects. The data is drawn from Refs. 12, 29, and 33–37.

$\times(\text{ET})_4\text{Fe}(\text{CN})_6 \cdot 3\text{H}_2\text{O}$ is in line with the proposed activated behavior of the 890 cm^{-1} mode. The 890 cm^{-1} feature follows the charge ordering in $\kappa\text{-(Et}_4\text{N)}(\text{ET})_4\text{Co}(\text{CN})_6 \cdot 3\text{H}_2\text{O}$ as well.

In the $\beta''\text{-(ET)}_2\text{SF}_5\text{RSO}_3$ family of isostructural systems, small changes in the chemical structure of the anion stabilize different phases including superconducting, metal-insulator, or metallic ground states.³⁵ The 890 cm^{-1} is very sensitive to this anion effect [Fig. 2(d)]. At 300 K, the 890 cm^{-1} mode shows a double structure $850/868\text{ cm}^{-1}$ for the superconductor ($R=\text{CH}_2\text{CF}_2$) and $844/862\text{ cm}^{-1}$ for the metal-insulator material ($R=\text{CHFCH}_2$), whereas a triplet is observed $843/868/881\text{ cm}^{-1}$ for the metallic compound ($R=\text{CHF}$). Such large differences are related to the structure and order within the anion pocket as well as details of intermolecular hydrogen bonding. The effect of chemical substitution in the $\beta''\text{-(ET)}_2\text{SF}_5\text{RSO}_3$ “tunable anion” materials is certainly much stronger than expected for normally infrared-active modes in materials with chemically different counterions, a result that supports the picture of EMV coupling. We note that the results for $\beta''\text{-(ET)}_2\text{SF}_5\text{RSO}_3$ are analogous to the large deuterium isotope shift that is a consequence of lattice effects involving interaction of ET ethylene groups and anions.¹¹ A positive isotope shift has also been predicted in this case.³⁹

Unusually strong temperature dependence of the 890 cm^{-1} mode was also found in the $\beta''\text{-(ET)}_2\text{SF}_5\text{CH}_2\text{SO}_3$ tunable anion organic conductor [Fig. 2(e)].³⁴ At room temperature the 890 cm^{-1} peak is almost invisible but it quickly develops a doublet structure at reduced temperature, a result that is related to two different oxidation states in the conducting ET layer. Similar behavior was also detected for some of the well-known totally symmetric features, such as the C=C motion, but not for normally activated (B_u) modes, indicating that the 890 cm^{-1} feature may be vibronically coupled as well.^{34,40} Splitting of 890 cm^{-1} peak is also observed in the $\beta\text{-(ET)}_2\text{I}_3$ superconductor and is attributed to structural modifications and superstructure formation.¹¹

The 890 cm^{-1} mode is sensitive to the formation of the superconducting state in several prototypical organic superconductors. Figure 2(f) displays the Raman resonance frequency of $\kappa\text{-(ET)}_2\text{Cu}[\text{N}(\text{CN})_2]\text{Br}$ as a function of temperature.³⁶ Under slow cooling conditions, a frequency increase of $\sim 2.2\text{ cm}^{-1}$ is found in the superconducting state. With rapid cooling, superconductivity is suppressed and no frequency shift is observed at T_c . The Raman response of $\alpha_r\text{-(ET)}_2\text{I}_3$ provides another example of the sensitivity of the 890 cm^{-1} mode to temperature.¹² It splits into two components at intermediate temperatures due to an incommensurate superstructure.^{12,41} The upper frequency component decreases by $\sim 1.7\text{ cm}^{-1}$ on cooling below T_c [Fig. 2(g)]. The trend at T_c is opposite in $\alpha_r\text{-(ET)}_2\text{I}_3$ and $\kappa\text{-(ET)}_2\text{Cu}[\text{N}(\text{CN})_2]\text{Br}$. No frequency shift is observed for the lower component in $\alpha_r\text{-(ET)}_2\text{I}_3$. Finally, we note that the 890 cm^{-1} mode is sensitive to the magnetic field-induced superconductor-to-normal state transition in $\kappa\text{-(ET)}_2\text{Cu}(\text{SCN})_2$.^{37,42} Figure 2(h) shows the 4 K reflectance ratio of $\kappa\text{-(ET)}_2\text{Cu}(\text{SCN})_2$ ($H_{c1} \sim 0.001\text{ T}$, $H_{c2} \sim 4.5\text{ T}$) compared with the response of the gold reference mirror. The

derivative-like line shape of the 17 T reflectance ratio spectra indicates a small but reproducible frequency shift between the superconducting and high-field normal states. The 890 cm^{-1} mode even more sensitive to H_{c2} in $\kappa\text{-(ET)}_2\text{Cu}[\text{N}(\text{CN})_2]\text{Br}$, where the ET building block molecule has an eclipsed distortion.⁴³

Taken together, the results in Fig. 2 point toward an unusual sensitivity of the 890 cm^{-1} mode to both physical and chemical tuning. This sensitivity, the observed red-shift between Raman and infrared response of $\kappa\text{-(Et}_4\text{N)}(\text{ET})_4\text{Co}(\text{CN})_6 \cdot 3\text{H}_2\text{O}$ [Figs. 2(a) and 2(b)] and $\kappa\text{-(ET)}_2\text{Cu}(\text{SCN})_2$,³⁸ and the fact that the 890 cm^{-1} feature is totally absent in the Raman spectrum of the neutral ET molecule and appears strongly in the Raman spectrum of the salts (which are more distorted)³⁸ support the proposed EMV-activated character of this feature and demonstrates the need for additional theoretical work to understand this activation. The recent results of Girlando *et al.*¹⁶ and Brake *et al.*³⁰ and the earlier studies of Demiralp and Goddard³¹ and Meneghetti *et al.*,³² involving dynamics calculations of the distorted ET molecule are a step in the right direction, as they account for the reduced symmetry of the ET building block molecule in the salts. For instance, reduction of local symmetry to D_2 yields 19 totally symmetric (A modes) and changes the eigenvector character quite substantially.^{16,32} Mode patterns for the four most strongly coupled modes are given in Ref. 16. In this rendering, the 890 cm^{-1} “ring breathing mode” is predicted to display strong vibronic coupling, and it is assigned as $\nu_{10}(A)$. Lower symmetry subgroups will obviously have slightly different naming schemes. For example, the 18 totally symmetric modes in the C_{2h} subgroup will have A_g symmetry, along with different eigenvector patterns.

Organic molecular solids exhibit cooperative effects over many different (and sometimes surprising) length, energy, and time scales.⁴⁴ Local distortions of the building block molecule (and the effect on EMV coupling) certainly goes to the heart of spectral interpretation, and molecular structure can influence electronic and transport processes as well. To cite just two examples, local structure may impact the detailed understanding of charge ordering in organic molecular conductors,⁴⁵ and disorder in the conformational degrees of freedom of the terminal ethylene groups has been predicted to influence T_c in the β_L and β_H phases of $(\text{ET})_2\text{I}_3$.⁴⁶

III. CONCLUSIONS

We report a detailed analysis of the vibrational response of several model organic molecular conductors and superconductors. Using both unpublished and literature data, we demonstrate that the 890 cm^{-1} mode displays an unusual sensitivity to both chemical and physical tuning effects for a wide variety of materials, suggesting that an electron-molecular vibrational mechanism is at work to activate the 890 cm^{-1} mode, among others, in ET-based organic molecular solids. According to a variety of crystallographic results as well as recent dynamics calculations, distortion of the ET building block molecule breaks local symmetry, and activates a different set of totally symmetric vibrational

modes.^{16,30–32} Thus, it is preferable to consider the 890 cm⁻¹ feature as a totally symmetric mode of a distorted ET molecule rather than as a ν_{60} (B_{3g}) mode of a perfectly flat (D_{2h}) model system. Consideration of nonplanar molecular symmetry also eliminates the need to invoke nonlinear coupling mechanisms. Increasingly complex dynamics simulations will certainly continue to provide an improved understanding of the mode character of various organic building block molecules. Local molecular distortions of the building block molecule may have important implications for the electronic character of organic solids as well.

ACKNOWLEDGMENTS

This project was supported at UT by NSF (Grant Nos. DMR-0139414 and INT-0086475). Work at the IMPPAS was supported within the EC (Grant No. G5MA-CT-2002-04049) and the PCSR (Grant No. 2004 - 2007). Efforts at ANL were supported by the DOE (MSD, BES: Grant No. W-31-109-ENG-38). Work at UBC was supported by NSERC (5-85653). We thank A. Girlando for access to unpublished results and useful discussions.

- ¹V. M. Yartsev and A. Graja, *Int. J. Mod. Phys. B* **12**, 1643 (1998).
- ²Y. M. Yartsev and R. Świetlik, *Rev. Solid State Sci.* **4**, 69 (1990).
- ³M. J. Rice, *Phys. Rev. Lett.* **37**, 36 (1976).
- ⁴M. J. Rice, L. Pietronero, and P. Brüesch, *Solid State Commun.* **21**, 757 (1977).
- ⁵M. J. Rice, V. M. Yartsev, and C. S. Jacobsen, *Phys. Rev. B* **21**, 3437 (1980).
- ⁶V. M. Yartsev, *Phys. Status Solidi B* **126**, 501 (1984).
- ⁷C. B. Duke, *Ann. N.Y. Acad. Sci.* **313**, 166 (1978).
- ⁸M. E. Kozlov, K. I. Pokhodnia, and A. A. Yurchenko, *Spectrochim. Acta, Part A* **43**, 323 (1987).
- ⁹J. E. Eldridge, C. C. Homes, J. M. Williams, A. M. Kini, and M.-H. Whangbo, *Spectrochim. Acta, Part A* **51**, 947 (1995).
- ¹⁰J. E. Eldridge, Y. Xie, H. H. Wang, J. M. Williams, A. M. Kini, and J. A. Schlueter, *Spectrochim. Acta, Part A* **52**, 45 (1996).
- ¹¹J. E. Eldridge, Y. Lin, J. Schlueter, H. H. Wang, and A. M. Kini, *Mol. Cryst. Liq. Cryst. Sci. Technol., Sect. A* **380**, 93 (2002).
- ¹²Y. Lin, J. E. Eldridge, J. Schlueter, H. H. Wang, and A. M. Kini, *Phys. Rev. B* **64**, 024506 (2001).
- ¹³M. G. Kaplunov and R. N. Lyubovskaya, *J. Phys. I* **2**, 1811 (1992).
- ¹⁴M. E. Kozlov and M. Tokumoto, *Synth. Met.* **70**, 1023 (1995).
- ¹⁵A. Girlando and A. Painelli, *Mol. Cryst. Liq. Cryst. Sci. Technol., Sect. A* **234**, 145 (1993).
- ¹⁶A. Girlando, M. Masino, A. Brillante, R. G. Della Valle, and E. Venuti, *Horizons in Superconductivity Research* (Nova Science Publishers, New York, 2003).
- ¹⁷Typical diffraction experiments measure electron (x-rays) or nuclear (neutrons) density, averaged both over time and over all unit cells of the crystal. Experimentally, the assignment of correct local symmetry and the quantification of distortions from the ideal D_{2h} prototype via crystal structure determination is hampered by several complications. (1) The ethylene group carbon atoms are often affected by conformational disorder, be it static or dynamic. In the dynamic case, an additional element of temperature dependence is introduced as the conformations freeze upon cooling the crystal. This disorder results in broadly peaked (or even split) density distributions, whose maximum (maxima) may be a poor measure of true atomic position. (2) ET molecules may be located on sites of higher crystallographic symmetry than is present locally, resulting in additional disorder. (3) More than one crystallographically independent ET molecule may be present in the structure. Thus, bulk structure determination is often advantageously employed in combination with a local probe such as optical spectroscopy.
- ¹⁸U. Geiser, A. J. Schultz, H. H. Wang, D. M. Watkins, D. L. Stupka, J. M. Williams, J. E. Schirber, D. L. Overmyer, D. Jung, J. J. Novoa, and M.-H. Whangbo, *Physica C* **174**, 475 (1991).
- ¹⁹U. Geiser, A. M. Kini, H. H. Wang, M. A. Beno, and J. M. Williams, *Acta Crystallogr., Sect. C: Cryst. Struct. Commun.* **47**, 190 (1991).
- ²⁰J. M. Williams, J. R. Ferraro, R. J. Thorn, K. D. Carlson, U. Geiser, H. H. Wang, A. M. Kini, and M.-H. Whangbo, *Organic Superconductors (Including Fullerenes): Synthesis, Structure, Properties, and Theory* (Prentice Hall, Upper Saddle River, NJ, 1992).
- ²¹A. J. Schultz, M. A. Beno, U. Geiser, H. H. Wang, A. M. Kini, J. M. Williams, and M.-H. Whangbo, *J. Solid State Chem.* **94**, 352 (1991).
- ²²N. Yoneyama, A. Higashihara, T. Sasaki, T. Nojima, and N. Kobayashi, *J. Phys. Soc. Jpn.* **73**, 1290 (2004).
- ²³U. Geiser and J. A. Schlueter, *Chem. Rev. (Washington, D.C.)* **104**, 5203 (2004).
- ²⁴U. Geiser, J. A. Schlueter, H. H. Wang, A. M. Kini, J. M. Williams, P. P. Sche, H. I. Zakowicz, M. L. Vanzile, J. D. Dudek, P. G. Nixon, R. W. Winter, G. L. Gard, J. Ren, and M.-H. Whangbo, *J. Am. Chem. Soc.* **118**, 9996 (1996).
- ²⁵J. A. Schlueter, B. H. Ward, U. Geiser, H. H. Wang, A. M. Kini, J. P. Parakka, E. Morales, H.-J. Koo, M.-H. Whangbo, R. W. Winter, J. Mohtasham, and G. L. Gard, *J. Mater. Chem.* **11**, 2008 (2001).
- ²⁶B. H. Ward, J. A. Schlueter, U. Geiser, H.-H. Wang, E. Morales, J. P. Parakka, S. Y. Thomas, J. M. Williams, P. G. Nixon, R. W. Winter, G. L. Gard, H.-J. Koo, and M.-H. Whangbo, *Chem. Mater.* **12**, 343 (2000).
- ²⁷P. Le Maguerés, L. Ouahab, N. Conan, C. J. Gómez-García, P. Delhaés, J. Even, and M. Bertault, *Solid State Commun.* **97**, 27 (1996).
- ²⁸P. Le Maguerés, Ph.D. thesis, Université de Rennes 1, Rennes, 1995.
- ²⁹R. Świetlik, A. Łapiński, L. Ouahab, and K. Yakushi, *C.R. Acad. Sci., Ser. IIc: Chim* **6**, 395 (2003).
- ³⁰K. Brake, B. J. Powell, R. H. McKenzie, M. R. Pederson, and T. Baruah, *J. Phys. IV* **114**, 293 (2004).
- ³¹E. Demiralp and W. A. Goddard III, *J. Phys. Chem. A* **102**, 2466 (1998).
- ³²M. Meneghetti, R. Bozio, and C. Pecile, *J. Phys. (France)* **47**, 1377 (1986).
- ³³R. Świetlik (unpublished).

- ³⁴B. Barszcz, Masters thesis, Polish University of Technology, Poznan, Poland, 2003.
- ³⁵B. R. Jones, I. Olejniczak, J. Dong, J. M. Pigos, Z. T. Zhu, A. D. Garlach, J. L. Musfeldt, H.-J. Koo, M.-H. Whangbo, J. A. Schlueter, B. H. Ward, E. Morales, A. M. Kini, R. W. Winter, J. Mohtasham, and G. L. Gard, *Chem. Mater.* **12**, 2490 (2000).
- ³⁶J. E. Eldridge, Y. Lin, H. H. Wang, J. M. Williams, and A. M. Kini, *Phys. Rev. B* **57**, 597 (1998).
- ³⁷I. Olejniczak, J. Choi, J. L. Musfeldt, Y. J. Wang, J. A. Schlueter, and R. A. Klemm, *Phys. Rev. B* **67**, 174502 (2003).
- ³⁸J. E. Eldridge, Y. Xie, Y. Lin, C. C. Homes, H. H. Wang, J. M. Williams, A. M. Kini, and J. A. Schlueter, *Spectrochim. Acta, Part A* **53**, 565 (1997).
- ³⁹A. Girlando (unpublished).
- ⁴⁰A. Szutarska, Masters thesis, Polish University of Technology, Poznan, Poland, 2001.
- ⁴¹ α_r -(ET)₂I₃ is a β -like phase, obtained from the thermal conversion of α -(ET)₂I₃.
- ⁴²Reflectance ratio spectra [$\Delta R=R(H)/R(H=0)$] were calculated to detect the small, field-dependent features.
- ⁴³R. Wesolowski, J. T. Haraldsen, J. Cao, J. L. Musfeldt, I. Olejniczak, J. Choi, Y. J. Wang, and J. A. Schlueter, *Phys. Rev. B* **71**, 214514 (2005).
- ⁴⁴R. T. Clay and S. Mazumdar, cond-mat/0406525 (to be published).
- ⁴⁵M. Dressel, N. Drichko, J. Schlueter, and J. Merino, *Phys. Rev. Lett.* **90**, 167002 (2003).
- ⁴⁶B. J. Powell, *J. Phys. IV* **114**, 363 (2004).